HPF1 remodels PARP1 active site for ADP-ribosylation of histones on serine

Cai-Hong Yun (yunch@pku.edu.cn)
Peking University https://orcid.org/0000-0002-5880-8307
Fa-Hui Sun
Peking University
Peng Zhao
Peking University
Nan Zhang
Center for Precision Medicine Multi-Omics Research, Peking University Health Science Center, Peking University
Lu-Lu Kong
Peking University
Catherine Wong
Center for Precision Medicine Multi-Omics Research, Peking University Health Science Center, Peking University

Article

Keywords: serine, HPF1, PARP1

Posted Date: September 18th, 2020

DOI: https://doi.org/10.21203/rs.3.rs-71025/v1

Version of Record: A version of this preprint was published at Nature Communications on February 15th, 2021. See the published version at https://doi.org/10.1038/s41467-021-21302-4.

Abstract

Upon binding to DNA breaks, poly(ADP-ribose) polymerase 1 (PARP1) ADP-ribosylates itself and other factors to initiate DNA repair. Serine is the major residue for ADP-ribosylation upon DNA damage, which strictly depends on HPF1. Here we report the crystal structures of human HPF1/PARP1-CAT ΔHD complex at 1.98 Å resolution and mouse and human HPF1 at 1.71 Å and 1.57 Å resolution, respectively. These structures and mutagenesis data confirm that the structural insights obtained in the HPF1/PARP2 study apply to PARP1. Moreover, we quantitatively characterize the key residues for HPF1/PARP1 binding. This information clarifies the confusion regarding HPF1/PARP1 assembly and can direct following functional studies. Our data show that through salt-bridging to Glu284/Asp286, Arg239 positions Glu284 for catalyzing serine ADP-ribosylation, maintains the local conformation of HPF1 to limit PARP1 automodification and facilitates HPF1/PARP1 binding through neutralizing the negative charge of Glu284. These findings and the high-resolution structural data may facilitate drug discovery targeting PARP1.

Introduction

Covalently attaching the ADP-ribose moiety from NAD^+ to substrate molecules (ADP-ribosylation, ADPr) is a reversible post-translational modification involved in various biological processes including DNA damage response (DDR), DNA replication, transcription, chromatin modulation, host-pathogen interactions, RNA metabolism, unfolded protein response and mitosis [1, 2, 3, 4]. The poly(ADP-ribose) polymerases (PARPs) family, also known as ADP-ribosyltransferase diphtheria toxin-like proteins (ARTDs), are the major enzymes catalyzing ADPr in eukaryotes [5]. Although 17 PARPs family members have been discovered, 80–90% of cellular NAD^+ consumption during DDR is related to the founding member PARP1, which plays an essential role in DNA damage repair [6, 7]. When DNA damage occurs, PARP1 can sense and attach to DNA chain breaks in milliseconds, which in turn activates its ADP-ribosyl transferase activity for auto-modification or modification of other factors including histones. The electronegative modifications further recruit other DDR machines to launch DNA repair. Due to its extensive and pivotal role in DDR, PARP1 has emerged to be a promising target in cancer treatment [8, 9, 10, 11, 12]. This is a highly active field of research, because of PARP1's relevance in many tumor types. Since 2014, several PARP1 inhibitors (such as olaparib and rucaparib) have been approved for the treatment of ovarian cancer, prostate cancer and breast cancer, based on the synthetic lethality strategy, and more inhibitors are being developed [13, 14, 15].

PARP1 consists of six domains [16, 17] (Supplemental Figure S1). Three zinc finger domains (Zn1, Zn2 and Zn3) are responsible for recognizing and binding to DNA breaks. The auto-modification domain (AD) contains a BRCA-C-terminus (BRCT) fold and bears multiple poly(ADP-ribosylation) sites. The Trp-Gly-Arg (WGR) domain interacts with Zn1, Zn3, CAT and DNA and is essential for coupling DNA binding to ADP-ribosyl transferase activation. The catalytic domain (CAT) contains two subdomains, HD and ART: The helical domain (HD) acts as an autoinhibitory domain in the folded state and undergoes local unfolding

upon PARP1 activation to enable NAD^+ binding and enzyme activation, while the ART domain catalyzes the transfer of ADP-ribose and is highly conserved in other ADP-ribosyl transferases (ARTs). In the last decade, several studies elegantly showed that an inter-domain interaction network is induced by the binding of DNA breaks to the zinc finger domains, which triggers conformational changes of the catalytic domain, especially the local unfolding of HD followed by complete exposure of the NAD^+ binding pocket in the catalytic core and PARP1 activation [18, 19, 20, 21, 22].

Besides the understanding of the intramolecular activation mechanism of PARP1, it is also necessary to clarify how other factors modulate PARP1 enzymatic output. A previously uncharacterized protein C4orf27 was demonstrated to be a cofactor of PARP1, which physically interacts with PARP1, restricts PARP1 hyper-automodification, promotes histone modification and changes the amino-acid specificity of ADP-ribosylation from aspartate/glutamate to serine [23, 24, 25]. This protein was therefore named histone PARylation factor 1 (HPF1). Soon afterwards, serine residue was proved to be the major target of PARP1 upon DDR [26]. These studies implied an important role played by HPF1 to regulate PARP1 function. Recently, Suskiewicz *et al.* determined the crystal structures of *Nematostella vectensis* and *Homo sapiens* HPF1 both at 2.09 Å resolution, and *Homo sapiens* HPF1/PARP2-CAT ΔHD complex at 2.96 Å resolution, which provided important insights into how HPF1 binding to PARP2 and promoting serine ADPr [27]. However, a high resolution structure of HPF1 in complex with PARP1, the most important member of PARPs was unavailable, and the resolution of the reported structures, especially HPF1/PARP2-CAT ΔHD complex, were modest. There also remain some unresolved questions related to the assembly and function of the complex. For example, why is Arg239 indispensable for the interaction between HPF1 and PARPs but this residue does not interact with any residue of PARPs? What functional roles does the conserved HPF1 Arg239 residue play? We have determined the crystal structures of mouse and human HPF1, and human HPF1/PARP1 complex at 1.71 Å, 1.57 Å and 1.98 Å resolution, respectively, and carefully studied the function of the key residues participating in HPF1/PARP1 interaction through extensive site-directed mutagenesis, ADPr activity assays, isothermal titration calorimetry (ITC) and mass spectrometry. Our work sheds light on the so far obscure role of Arg239 in regulating complex assembly and function, and the high resolution HPF1/PARP1 complex structure will facilitate future drug design on this important target.

Results

HPF1 binds to activated ART domain of PARP1

HPF1 has been shown to bind to the CAT domain (HD-ART) of PARP1 in cells in response to DNA damage [23]. Since HD is an autoinhibitory domain that blocks productive binding to NAD^+ in the resting state, and it undergoes local unfolding to enable NAD^+ binding and ADP-ribose transferase activity when PARP1 binds to DNA breaks [19], we asked if unfolding or removing the HD subdomain is the prerequisite for HPF1 binding to PARP1. To answer this question, we tested HPF1 binding to PARP1 CAT domain in the full-length autoinhibited form or in the constitutively activated form through removing the majority (residues

679-786) of the autoinhibitory domain HD (CAT ΔHD) using size-exclusion chromatography (SEC). Interestingly, it is observed that CAT ΔHD, but not full-length CAT, forms a complex with HPF1 (Figure 1a). The interaction was further quantitatively characterized by isothermal titration calorimetry (ITC), which showed that CAT ΔHD binds to HPF1 with a dissociation constant (K_d) of about 1.5μM and 1:1 stoichiometry (Figure 1b, Table 1, Supplemental Figure S2,S3), while full-length CAT showed no binding to HPF1 (Figure 1c). Since these observations confirmed that HPF1 binds to activated CAT, we also tested the binding of HPF1 to full-length PARP1 activated by DNA (Table 1, Supplemental Figure S2). HPF1 binds to full-length PARP1 with a K_d of about 2.8μM, slightly weaker than its binding affinity for CAT ΔHD, probably related to transient folding of the HD domain in solution.

The human HPF1/PARP1-CAT ΔHD Complex crystal structure

In order to understand the assembly and function of the HPF1/PARP1 complex, the crystal structure of human HPF1/PARP1-CAT ΔHD complex bound by benzamide (introduced when expressing the protein) was determined and refined to 1.98 Å (Figure 2a, Supplemental Figure S4 and Table S1). HPF1 and PARP1 were confirmed to form a 1:1 complex since there were one HPF1 and one PARP1-CAT ΔHD molecule in the asymmetric unit of the complex crystal structure.

The high resolution structure of the HPF1/PARP1-CAT ΔHD complex reveals an extensive interface between the two proteins that envelopes the region of the PARP1 active site (see interface I in Figure 2a). The hetero-dimer binding interface was confirmed through extensive mutagenesis combined with ADP-ribosylation assay and ITC assay. It has been well established that HPF1 binding to PARP1 restricts hyper-automodification of PARP1 [23, 26]. Indeed, hyper-automodification of PARP1 showed up clearly on SDS-PAGE as smeared bands above the un-modified PARP1 band, while wild-type HPF1 binding abolished this effect (Figure 2b, see lanes 3 and 4). On the designated hetero-dimer interface, HPF1 Phe268, Phe280, Asp283, Cys285 and Lys307 are found to directly interact with PARP1 residues (Figure 2a, top-right and bottom-right insets), and these residues are conserved in HPF1 from different species (Supplemental Figure S5). Indeed, mutating most of these HPF1 residues (F268S, F280A, D283H, C285H and K307S) significantly restored hyper-automodification of PARP1 (Figure 2b, see lanes 9, 11, 12, 14 and 15), indicating loss of binding between the HPF1 mutants and PARP1. ITC assays further confirmed that these mutations dramatically reduced the binding affinity between HPF1 and PARP1-CAT ΔHD (Table 1, Supplemental Figure S2, S3). Importantly, HPF1 F268S and D283H mutations completely abolished the interaction between these two proteins, which may be used in following functional studies on the HPF1/PARP1 system. Interestingly, although PARP1, PARP2 and PARP3 share pretty high sequence homology in the CAT domain (25.41% of the sequences are identical and the other 18.85% are strongly similar), PARP3 lacks the key residues corresponding to His826, Leu985, Ser1012, Leu1013 and Trp1014 in PARP1, which according to the HPF1/PARP1-CAT ΔHD complex structure and the mutagenesis data are important for HPF1-PARP interaction, while these key residues are largely conserved between PARP1

and PARP2 (Figure 2c, Supplemental Figure S6). This explains why HPF1 can bind to PARP1 and PARP2, but not to PARP3 [23].

In examining the structure, we noted another interface between a different HPF1 and PARP1 molecule in the crystal lattice (see interface II in Figure 2a, top-left inset). However, mutating key residues on this interface (Glu138, Phe139 and Lys216) did not interfere with the binding (Figure 2b, see lanes 5, 6, 7; Table 1, Supplemental Figure S2, S3), and these residues are not conserved in HPF1 (Supplemental Figure S5). Thus this contact does not appear to be relevant to the catalytic function of the HPF1/PARP1 complex.

We also determined structures of human and mouse HPF1 alone, and that the conformation does not change upon formation of the complex with PARP1 (see Supplemental Figure S7). Notably, analysis of the surface electrostatic potential showed that positively and negatively charged areas are evenly distributed on the surface of this protein, except for part of helix α9/α10 and the linker loops connecting helices α6 and α7, where the protein surface is dominantly negatively charged (Supplemental Figure S7B).

HPF1 binding remodels the PARP1 active site for histone binding and serine ADPr

Remarkably, our functional analysis of the structure shows that HPF1 and PARP1 form a composite active site, with HPF1 contributing key active site residues.

We first analyzed the surface electrostatic potential of HPF1, PARP1-CAT ΔHD and the complex (Figure 3a). Though PARP1 has been shown to play a key role in DDR involving the modification of histones [16, 28], the surface of ART subdomain, especially the active site, is positively charged, which is clearly incompatible with the positively charged nucleosome (Supplemental Figure S8). Interestingly, HPF1 binding to PARP1-CAT dramatically changes the situation. As is mentioned above, HPF1 surface covering helix α9, α10 and the loops connecting helices α6 and α7 is negatively charged (Supplemental Figure S7). Many solvent-exposed acidic amino-acid residues are located in this region, including Asp235, Glu240, Glu243, Asp245, Glu273, Asp283, Glu284, Asp286 and Glu292, and Arg239 turns out to be the only basic residue in this region (Figure 3a). Notably, Arg239 and most of these acidic residues are conserved in HPF1 from different species (Supplemental Figure S5). When binding to PARP1, this negatively charged region of HPF1 merges to the active site of PARP1-ART and changes the surface potential of the latter, creating an overall negatively charged joint active site that would accommodate the access of the positively charged histones (Figure 3a). The surface of the HD subdomain facing the active site is also negatively charged due to three acidic residues Glu756, Asp766 and Asp770 and lack of any basic residue here, hence seems to form a negatively charged narrow tunnel with the joint active site (Figure 3b). However, the HD subdomain is believed to undergo partial unfolding upon PARP1 activation [19], and therefore it is unknown whether the tunnel still maintains. We speculate that if the HD subdomain does not completely unfold, the negatively charged tunnel may still maintain (but likely undergoes some

conformational changes) that is presumably most accessible for positively charged extended peptide substrate (say histone H3 N-terminal tail), while the folded and/or negatively charged proteins may not readily access this joint active site to get ADP-ribosylated.

A benzamide molecule was found to bind in the active center of the HPF1/PARP1-CAT ΔHD complex structure (Supplemental Figure S4). When superimposed with the previously reported PARP1-CAT ΔHD/BAD complex crystal structure (PDB 6BHV) [22], the benzamide molecule in our HPF1/PARP1-CAT ΔHD complex structure well overlaps the benzamide moiety of BAD, the NAD^+ analog (Figure 3c). Importantly, we noted that the HPF1 Glu284 side-chain carboxyl, being positioned/locked by the Arg239-Glu284 salt-bridge, is located beside the ribose of the ADP moiety of carba-NAD^+ (representing the acceptor for ADP-ribosylation [29], see Figure 3d), and is about 1.9Å farther away than the latter from the C1" atom of the nicotinamide ribose moiety of BAD/NAD^+ (representing the donor for ADP-ribosylation, see Figure 3c), which from the structural biological view would strongly suggest an important functional role of this residue rather as a catalyzer for ADP-ribose transfer to a third party (say a serine residue) than as a direct acceptor itself for ADP-ribose. In NAD^+, the positively charged nicotinamide nitrogen trends to deprive an electron from the connecting ribose C1" carbon, rendering the latter an oxacarbenium ion that would then be attacked by a nucleophile such as a negatively charged/deprotonated amino-acid side-chain. Since acidic amino-acids glutamate and aspartate may spontaneously lose a proton to become negatively charged at physiological pH, these residues can be readily ADP-ribosylated once they access the active center of ART (for example, in the absence of HPF1, see Figure 3e). However, in the HPF1/PARP1-CAT ΔHD complex structure the Glu284 side-chain carboxyl is too far away (~4.6Å) from the NAD^+ to attack the ribose C1" carbon (Figure 3c). Therefore it seems unlikely that Glu284 itself can get ADP-ribosylated. On the other hand, since the non-acidic serine residue does not spontaneously lose a proton at physiological pH, it must be activated (deprotonated) by a third party prior to ADP-ribosylation. The Glu284 side-chain carboxyl may fulfill this task when it becomes negatively charged (Figure 3f). Indeed, mutating HPF1 Glu 284 to Alanine (E284A) completely abolished ADP-ribosylation of histones (Figure 2b, lane 13). The same observation and proposal of function have been made by Suskiewicz *et al.* in their structural studies of HPF1/PARP2-CAT ΔHD structure and functional studies including PARP1 and PARP2 [27].

Why does HPF1 binding hinder PARP1 automodification and poly-ADP-ribosylation?

Based on the verified interaction mode between HPF1 and PARP1-CAT ΔHD (corresponding to interface I shown in Figure 2a), an overall model of HPF1 binding to full-length activated PARP1 except the Zn2 and AD domains is proposed through overlapping the PARP1-ART domain with the corresponding domain in the PARP1/DNA complex structure (PDB 4DQY) (Figure 4a) [18]. HPF1 binds to ART at the active site of the enzyme, while in the meanwhile it is well accommodated with other domains of PARP1 except for HD that undergoes local unfolding upon PARP1 activation. This model immediately hints why HPF1 binding

restricts automodification of PARP1. According to the previous model proposed by Langelier *et al.*, the AD/BRCT domain carrying most of the automodification sites is located close to the CAT domain presumably for being ADP-ribosylated [18] (Supplemental Figure S1). This location is roughly the same place where HPF1 binds (compare Figure 4a to Supplemental Figure S1). We therefore speculate that HPF1 binding would dislodge AD from this location, hence limits the automodification of PARP1, at least in the folded BRCT domain.

The complex structure hints that HPF1 not only restricts hyper-automodification of PARP1, but may limit the modification from poly-ADP-ribosylation to mono-ADP-ribosylation. An early study by Ruf *et al.* observed the ADP moiety of carba-NAD^+ binding in the active site, and this ADP moiety was believed to represent the acceptor for the next ADP-ribose during poly-ADP-ribose chain elongation and branching [29]. Comparing to the HPF1/PARP1-CAT ΔHD complex structure reported here, we noted that the ADP (*i.e.* the acceptor for next ADP-ribose in poly-ADP-ribosylation) binding site is partly occupied by HPF1 residues Asp283 and Glu284 (Figure 3d), which would implicate that HPF1 binding is likely to prevent poly-ADP-ribose chain elongation and branching. However, we speculate that poly-ADP-ribosylation may still take place, likely at lower probability, due to the relatively weak and thus transient binding between HPF1 and PARP1. This explains the long smeared bands observed in our ADP-ribosylation assay (Figure 2b, see histone $H3/H4^{ADPr}$).

The unique role of HPF1 Arg239

Arg239 is highly conserved in HPF1 (Supplemental Figure S5), and has been thought to be important for the interaction between HPF1 and PARPs. Mutating this residue to alanine (R239A) did restore automodification of PARP1 (Figure 2b, lane 8), which was previously interpreted to be loss of binding between HPF1 and PARP1 [23].

However, in the human HPF1/PARP1-CAT ΔHD and HPF1/PARP2-CAT ΔHD complex structures, HPF1 Arg239 was found to only interact with Glu284 and Asp286, but not with any residue from PARP1/2 (Figure 4b). Furthermore, ITC assays confirmed that this mutation only mildly weakens the binding affinity between HPF1 and PARP1, indicating that without Arg239 HPF1 still binds pretty well to PARP1 (Table 1). Curiously, in the ADP-ribosylation assays, the band of HPF1 R239A, but not of any other HPF1 mutants, clearly shifted on the SDS-PAGE (Figure 2b, lane 8, black arrow), which looks very likely that HPF1 R239A itself was ADP-ribosylated. We then analyzed the shifted HPF1 R239A band by Mass Spectrometry, which confirmed that HPF1 R239A did get ADP-ribosylated on Asp235 and Glu240, two acidic residues located on both sides of residue 239 in the long loop connecting helices α6/α7 (Figure 4b, 4c). The long loop regions are often difficult to resolve in crystal structure due to their intrinsic flexibility, but in HPF1 the long loop connecting helices α6 and α7 (residues 217-244) is ordered and well resolved. As is shown in Figure 4b, the C-terminal half of this long loop is stabilized by two groups of interactions: one is the salt-bridge network including Arg239-Asp286 and Arg239-Glu284, which also acts to position

the catalytically important Glu284 side-chain; the other is the hydrophobic interaction between Tyr238 phenyl and Val218 side-chain, and hydrogen bond between Tyr238 hydroxyl and Glu292 carboxyl. It is inferred that when Arg239 was mutated to alanine that lost the interlocking with Glu284 and Asp286, the loop became so flexible that Asp235 and Glu240 gained the freedom to attack NAD^+ in the active center and became ADP-ribosylated. Importantly, although HPF1 R239A still bound PARP1 pretty well, it also restored the automodification of PARP1 (Figure 2b, lane 8). The PARP1 automodification domain (AD) contains a folded subdomain BRCT (residues 380-480) and an unstructured automodification peptide (residues 481-530). In a previous *in vitro* ADP-ribosylation assay, the serine residues in the Lys-Ser motif within the automodification peptide (Ser499, Ser507and Ser519), but not that in the BRCT subdomain (Lys467-Ser468), were ADP-ribosylated [24] in the presence of HPF1, indicating that the Lys-Ser motif in a flexible peptide, but not in a folded domain may access the remodeled HPF1/PARP1 active center under certain circumstances. In our assays, HPF1 WT binding robustly limited automodification of PARP1, while R239A, although still bound to PARP1, restored the automodification. Taken together, our data indicate that the rigidity of the loop region strengthened by Arg239-Glu284/Arg239-Asp286 interactions is essential for limiting PARP1 automodification in the unstructured automodification peptide region.

In the ADP ribosylation assay we also noted that the HPF1 E284A band mysteriously became weaker (Figure 2b, lane 13, gray arrow), indicating losing a small amount of the un-modified protein (or ADP-ribosylation of a small portion of the protein). However, the modification of this mutant HPF1 protein must be very minor since no shifted band was obviously seen on the gel. We speculate that in this mutant, after losing the Arg239-Glu284 salt-bridge but still maintaining the Arg239-Asp286 salt-bridge, the loop region gained some flexibility but the acidic residues (say Asp239 and Glu240) did not gain enough freedom to attack NAD^+ to be ADP-ribosylated. Accordingly, HPF1 E284A only mildly restored PARP1auto-modification, which again supported the notion that the rigidity of this loop region strengthened by Arg239-Glu284/Arg239-Asp286 interactions is essential for limiting PARP1 automodification.

Why is HPF1 Arg239 important for HPF1/PARP1 binding?

The above observations do not explain why mutating Arg239 to alanine weakens the interaction between HPF1 andPARP1, since no residue in the loop region (including Arg239 itself) directly interacts with PARP1. We noted that the HPF1 E284A mutation showed a very unique behavior in our assays. It is the only mutation that enhanced the binding between HPF1 and PARP1 (Table 1). Taken into account the negative electrostatic property of the joint active site discussed above, we propose that the existence of the negatively charged Glu284 in the active center is not favorable for HPF1/PARP1 binding, while the salt-bridge with the positively charged Arg239 side-chain may act to neutralize the negative charge on Glu284 carboxyl, thus facilitate the binding. Mutating Arg239 to directly break Arg239-Glu284 interaction, or mutating Tyr238 to destroy the local conformation supporting Arg239-Glu284 interaction, would restore the negative charge of Glu284, thus weaken HPF1/PARP1 binding. This explains why HPF1

R239A (and/or Y238A, as was found in the previous study [23]) mutation weakens the binding between the two proteins, and indicates that although mutating Arg239 (and/or Tyr238) may apparently weaken HPF1/PARP1 binding, they may not be the right choices to act as the non-binding control in functional studies because the mutation(s) lead to much more complicated consequences rather than simply abolishing the binding – and, they do not really abolish the binding.

Taken together, our study indicates that Arg239 is a key residue acting to 1) position Glu284 at the right location for catalyzing serine ADP-ribosylation; 2) stabilize the conformation of the long loop region across Arg239 to limit auto-modification of PARP1; 3) facilitate HPF1/PARP1 binding through neutralizing the negative charge of Glu284 side-chain.

Discussion

The sea anemone and human HPF1 (both at 2.09 Å resolution) and human HPF1/PARP2-CAT ΔHD complex (at 2.96 Å resolution) structures determined by Suskiewicz *et al*. provided the first glance at the interaction between HPF1 and a PARP family member. This work depicted the mechanism about how this binding completes the PARP2 active site and promotes ADP-ribosylation of histone serine, which were believed to also apply to PARP1 based on the NMR and functional studies [27]. Our studies independently determined at higher resolution the crystal structures of mouse and human HPF1 (at 1.71 Å and 1.57 Å resolution, respectively) and human HPF1/PARP1-CAT ΔHD complex (at 1.98 Å resolution), which provided direct structural insights into how HPF1 binds to PARP1, why HPF1 prefers binding to PARP1/2 but not PARP3, why this interaction limits hyper-automodification of PARP1/2 and may also limit poly-ADP-ribosylation. The HPF1/PARP1-CAT ΔHD complex also provided insights into why HPF1 binding promotes histone peptide recognition and serine ADP-ribosylation. Since PARP1 and PARP2 share pretty high homology in the CAT domain (45.7% identity), the Suskiewicz *et al*. structures and ours look similar (Supplemental Figure S9), and our structural and functional studies confirmed most of the proposals made by Suskiewicz *et al*.

Besides confirming the key findings by Suskiewicz *et al*., our work provides novel and fundamental insights into the structure-function relationships of the HPF1/PARP1 complex. Since there are always multiple contacting interfaces due to protein molecules packing in crystals, and the packing may distort the protein complex architecture, caution must be taken to carefully verify which observed interface in the complex crystal structure represents the true dimer interface in solution. As a common practice in crystallography, this is usually done by extensive mutagenesis combined with functional studies, which were absent in the previous study, but are fulfilled in our study. When studying the function of HPF1 mutants to verify the true dimer interface, we not only conducted the traditional ADP-ribosylation assays (Fig. 2b), an indirect and non-quantitative way to ask if the HPF1/PARP1 complex is formed, but also carefully measured the K_d values using ITC assays (Table 1). Our data quantitatively and directly described the binding behavior between HPF1 and PARP1, and showed that only certain mutations (F268S and D283H) can completely abolish the binding, which may be used in following functional

studies, especially in the cell-based studies, as non-binding control. While if using other mutations, the experimental readout may be confusing or even misleading.

One such confusing and misleading result is related to HPF1 Arg239. In the previous studies, this residue was thought to mediate HPF1 and PARP1/2 interaction, but this idea is not supported by the structures. The same confusion applies to Tyr238, too, a residue located inside the HPF1 molecule. To resolve this problem, we first asked if Arg239 interacts with some other PARP1 residue not presenting in our HPF1/PARP1-CAT ΔHD complex structure. Based on the structural model (Fig. 4a), the PARP1 HD subdomain seems to be the only domain that could directly interact with HPF1 Arg239, and Glu756 in the HD subdomain seems to be the residue most likely to form a salt-bridge with HPF1 Arg239. However, it has been proved that the HD subdomain hinders the binding of HPF1, and our mutagenesis studies on PARP1 E756A showed that this mutation had no effect on HPF1/PARP1 binding (Supplemental Figure S2). On the other side, the ITC data confirmed that HPF1 R239A still binds to PARP1, and Mass Spectrometry confirmed that this mutant protein got ADP-ribosylated in the ADP-ribosylation assay. Taken into account the observation that HPF1 R239A significantly restored PARP1 automodification, we propose that Arg239 (and presumably also Tyr238) acts at the central stage to stabilize the local conformation of the α6-to-α7 loop region through interlocking with Glu284 and Asp286 (and through intramolecular interactions for Tyr238), which is essential for limiting PARP1 automodification, but dispensable for histone serine modification. To our surprise, HPF1 E284A mutant binds to PARP1-CAT ΔHD with about 3 times higher affinity than HPF1 WT, which hints that the acidic property of Glu284 is not favored for HPF1/PARP1 binding and that neutralizing the negative charge of Glu284 by Arg239 facilitates the binding. In accordance with the observation on HPF1 R239A that loses the Arg239-Glu284 and Arg239-Asp286 salt-bridges, the HPF1 E284A mutant, losing only the Arg239-Glu284 salt-bridge, only partly restored PARP1 automodification (Fig. 2b), which once again supports our proposal about the Arg239 function of stabilizing the local conformation to limit PARP1 automodification. Since the function of Arg239 is much more complicated than it was previously proposed, if one use this mutation as a control to abolish HPF1 and PARP1/2 binding in cell-based studies, the result may be misleading.

Taken together, our work provided the direct glance of the complex between HPF1 and PARP1, the most important member of the PARP family. The higher resolution structures, along with the extensive mutagenesis studies and quantitative functional study data in our work, completed the previous studies done by Suskiewicz *et al*. and clarified the suspending questions in their studies. The discoveries made by Suskiewicz *et al*. and us would have important implications in drug discovery targeting PARP1/2. Since histone serine ADP-ribosylation is a key step in DDR [8, 9, 13, 16, 26], and turning off PARP1/2 activity to inhibit DNA damage response in tumor cells is a promising approach in treating cancers, it is important that drug discovery targeting PARP1/2 should consider inhibiting HPF1-dependent histone serine ADP-ribosylation, *i.e.* consider the remodeled active site structure, instead of the open active site of PARP1/2 alone.

Declarations

AUTHOR CONTRIBUTIONS

C.-H.Y. instructed the project. F.H.S. and P.Z. designed and performed the crystallographic and functional experiments. N. Z. and C.C.L.W. conducted the Mass Spectrometry studies. F.H.S., C.C.L.W. and C.H.Y. analyzed the data and wrote the manuscript.

ACKNOWLEDGMENTS

We thank the staffs of APS beamline ID-19 and SSRF beamlines BL18U/BL19U1 for assistance in data collection. We thank Prof. Jia-Dong Wang for providing the PARP1 cDNA. We thank Drs. Michael J Eck, Oreste Segatto and Jianming Zhang for helpful discussion. This study was funded by the National Natural Science Foundation of China (No. 31270769), the National Basic Research Program of China (973 Program, No. 2012CB917202), and the Ministry of Science and Technology of China (NCET-12-0013).

Tables

Table 1. Dissociation constant (K_d) of HPF1 mutants binding to PARP1 CAT ΔHD and their effects on ADP-ribosylation of full-length PARP1 (automodification), histone H3 and HPF1.

Location of HPF1 mutants		K_d(μM)[1]	ADP-ribosylation[2]		
			PARP1	H3	HPF1
Control	wild-type	1.5±0.2	-	++	-
		2.8±0.3[3]			
Interface I[4]	F268S	N.D.	+++	++	-
	F280A	6.0±0.8	+++	++	-
	D283H	N.D.	+++	+	-
	C285H	28.7±1.6	+++	++	-
	K307S	9.3±1.2	++	++	-
Interface II[4]	E138K	1.7±0.1	-	++	-
	F139S	2.4±0.1	-	++	-
	K216E	1.4±0.1	-	++	-
Active center	R239A	2.4±0.1	+++	+	+++
	E284A	0.3±0.0	+	-	+

[1] K_d data were determined in isothermal titration calorimetric (ITC) assays. The measurements were conducted in duplicates and the standard error values were listed. See Supplemental Figure S2 and S3 for raw data.

[2] The assessment was made based on the ADP-ribosylation assays (see Figure 2b). Number of "+" indicates the relative intensity of observed ADP-ribosylation.

[3] Titration of HPF1 to full-length PARP1 in the presence of DNA. Other K_d values listed in this table are for titration of HPF1 to PARP1-CAT ΔHD.

[4] These interfaces were observed in the HPF1/PARP1-CAT ΔHD complex structure, indicating the two candidate interaction modes between HPF1 and PARP1.

References

1. Palazzo L, Mikoc A, Ahel I. ADP-ribosylation: new facets of an ancient modification. *FEBS J* **284**, 2932–2946 (2017).
2. Gupte R, Liu Z, Kraus WL. PARPs and ADP-ribosylation: recent advances linking molecular functions to biological outcomes. *Genes Dev* **31**, 101–126 (2017).
3. Barkauskaite E, Jankevicius G, Ladurner AG, Ahel I, Timinszky G. The recognition and removal of cellular poly(ADP-ribose) signals. *FEBS J* **280**, 3491–3507 (2013).
4. Crawford K, Bonfiglio JJ, Mikoc A, Matic I, Ahel I. Specificity of reversible ADP-ribosylation and regulation of cellular processes. *Crit Rev Biochem Mol Biol* **53**, 64–82 (2018).
5. Hottiger MO, Hassa PO, Luscher B, Schuler H, Koch-Nolte F. Toward a unified nomenclature for mammalian ADP-ribosyltransferases. *Trends Biochem Sci* **35**, 208–219 (2010).
6. Bian C, *et al.* NADP(+) is an endogenous PARP inhibitor in DNA damage response and tumor suppression. *Nature communications* **10**, 693 (2019).
7. Krietsch J, *et al.* Reprogramming cellular events by poly(ADP-ribose)-binding proteins. *Mol Aspects Med* **34**, 1066–1087 (2013).
8. Farmer H, *et al.* Targeting the DNA repair defect in BRCA mutant cells as a therapeutic strategy. *Nature* **434**, 917–921 (2005).
9. Bryant HE, *et al.* Specific killing of BRCA2-deficient tumours with inhibitors of poly(ADP-ribose) polymerase. *Nature* **434**, 913–917 (2005).
10. Jagtap P, Szabo C. Poly(ADP-ribose) polymerase and the therapeutic effects of its inhibitors. *Nat Rev Drug Discov* **4**, 421–440 (2005).
11. Fong PC, *et al.* Inhibition of poly(ADP-ribose) polymerase in tumors from BRCA mutation carriers. *N Engl J Med* **361**, 123–134 (2009).
12. Helleday T. The underlying mechanism for the PARP and BRCA synthetic lethality: clearing up the misunderstandings. *Mol Oncol* **5**, 387–393 (2011).
13. Vyas S, Chang P. New PARP targets for cancer therapy. *Nat Rev Cancer* **14**, 502–509 (2014).
14. Jain PG, Patel BD. Medicinal chemistry approaches of poly ADP-Ribose polymerase 1 (PARP1) inhibitors as anticancer agents - A recent update. *Eur J Med Chem* **165**, 198–215 (2019).
15. Steffen JD, *et al.* Targeting PARP-1 allosteric regulation offers therapeutic potential against cancer. *Cancer Res* **74**, 31–37 (2014).

16. Ray Chaudhuri A, Nussenzweig A. The multifaceted roles of PARP1 in DNA repair and chromatin remodelling. *Nat Rev Mol Cell Biol* **18**, 610–621 (2017).
17. Langelier MF, Eisemann T, Riccio AA, Pascal JM. PARP family enzymes: regulation and catalysis of the poly(ADP-ribose) posttranslational modification. *Curr Opin Struct Biol* **53**, 187–198 (2018).
18. Langelier MF, Planck JL, Roy S, Pascal JM. Structural basis for DNA damage-dependent poly(ADP-ribosyl)ation by human PARP-1. *Science* **336**, 728–732 (2012).
19. Dawicki-McKenna JM, *et al.* PARP-1 Activation Requires Local Unfolding of an Autoinhibitory Domain. *Mol Cell* **60**, 755–768 (2015).
20. Eustermann S, *et al.* Structural Basis of Detection and Signaling of DNA Single-Strand Breaks by Human PARP-1. *Mol Cell* **60**, 742–754 (2015).
21. Langelier MF, Planck JL, Roy S, Pascal JM. Crystal structures of poly(ADP-ribose) polymerase-1 (PARP-1) zinc fingers bound to DNA: structural and functional insights into DNA-dependent PARP-1 activity. *J Biol Chem* **286**, 10690–10701 (2011).
22. Langelier MF, Zandarashvili L, Aguiar PM, Black BE, Pascal JM. NAD(+) analog reveals PARP-1 substrate-blocking mechanism and allosteric communication from catalytic center to DNA-binding domains. *Nature communications* **9**, 844 (2018).
23. Gibbs-Seymour I, Fontana P, Rack JGM, Ahel I. HPF1/C4orf27 Is a PARP-1-Interacting Protein that Regulates PARP-1 ADP-Ribosylation Activity. *Mol Cell* **62**, 432–442 (2016).
24. Bonfiglio JJ, *et al.* Serine ADP-Ribosylation Depends on HPF1. *Mol Cell* **65**, 932–940 e936 (2017).
25. Leidecker O, *et al.* Serine is a new target residue for endogenous ADP-ribosylation on histones. *Nat Chem Biol* **12**, 998–1000 (2016).
26. Palazzo L, Leidecker O, Prokhorova E, Dauben H, Matic I, Ahel I. Serine is the major residue for ADP-ribosylation upon DNA damage. *Elife* **7**, (2018).
27. Suskiewicz MJ, *et al.* HPF1 completes the PARP active site for DNA damage-induced ADP-ribosylation. *Nature* **579**, 598–602 (2020).
28. Messner S, *et al.* PARP1 ADP-ribosylates lysine residues of the core histone tails. *Nucleic Acids Res* **38**, 6350–6362 (2010).
29. Ruf A, Rolli V, de Murcia G, Schulz GE. The mechanism of the elongation and branching reaction of poly(ADP-ribose) polymerase as derived from crystal structures and mutagenesis. *J Mol Biol* **278**, 57–65 (1998).

Figures

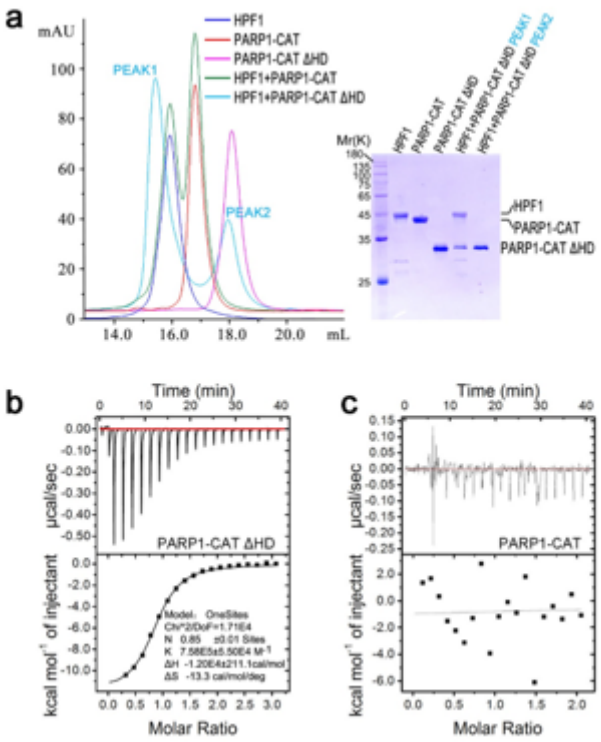

Figure 1

HPF1 binds to PARP1-CAT ΔHD. (a) SEC assay indicated that HPF1 binds to PARP1-CAT ΔHD, but not full-length PARP1-CAT. (b) Typical ITC data where human HPF1 was titrated into PARP-1 CAT ΔHD. In this titration the association constant (K) of HPF1/PARP-1 CAT ΔHD was estimated to be 7.58E5±5.50E4 M-1, equivalent to a dissociation constant (Kd) about 1.3μM. After replicated measurements the final Kd value was determined to be 1.5±0.2μM (Table 1, Supplemental Figure S2). (c) Typical ITC data where human HPF1 was titrated into full-length PARP-1 CAT. No binding was detected in this assay.

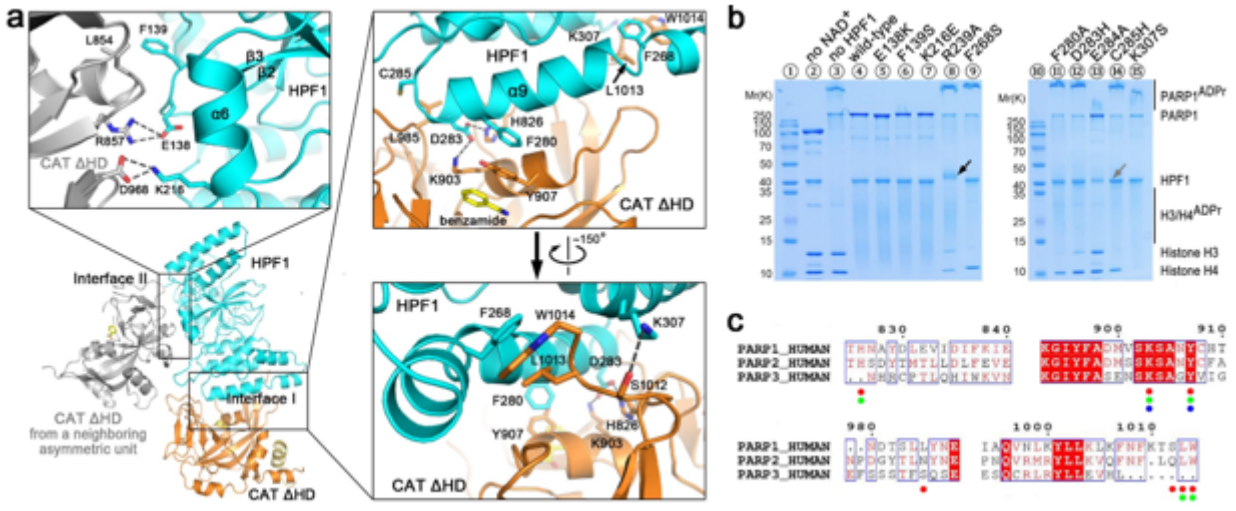

Figure 2

Crystal structure of human HPF1/PARP1-CAT ΔHD and the binding mode between these two proteins. (a) Overall structure and the interaction details between human HPF1 and PARP1-CAT ΔHD. The overall structure of human HPF1/PARP1-CAT ΔHD was shown as cartoons. HPF1 and PARP1-CAT ΔHD are colored in cyan and orange, respectively. The gray-colored molecule on the left side indicates another PARP1-CAT ΔHD molecule from a neighboring crystallographic asymmetric unit that also contacts the HPF1 molecule shown here due to close packing of molecules in the crystal. Therefore, the complex crystal structure actually indicated two possible interaction modes between HPF1 and PARP1-CAT ΔHD. The three insets show the key residues on the two interaction interfaces that mediate the interactions between the HPF1 and PARP1 in the crystal. The dashes indicate polar interactions between the key residues. (b) Mutagenesis/ADP ribosylation studies to verify which key residues indicated in crystal structure do mediate HPF1 and PARP1 binding in solution. Hyper-automodification of PARP1 (shown by the smeared PARP1ADPr bands on SDS-PAGE) was recognized as the sign of losing the interaction between HPF1 mutants and PARP1. Surprisingly, we noted that HPF1 R239A, but not any other HPF1 mutants, was robustly ADP-ribosylated in the assay (black arrow, and see Figure 4c), while E284A seemed to be mildly ADP-ribosylated – The HPF1 E284A band became weaker, indicating loss of un-modified protein in the assay (gray arrow). (c) Amino-acid sequence alignment of human PARP1/2/3. The verified key residues to mediate HPF1 binding in PARP1 in solution are indicated by red dots. The corresponding residues in PARP2 and PARP3, if they are conserved (same to those in PARP1), are indicated by green and blue dots, respectively.

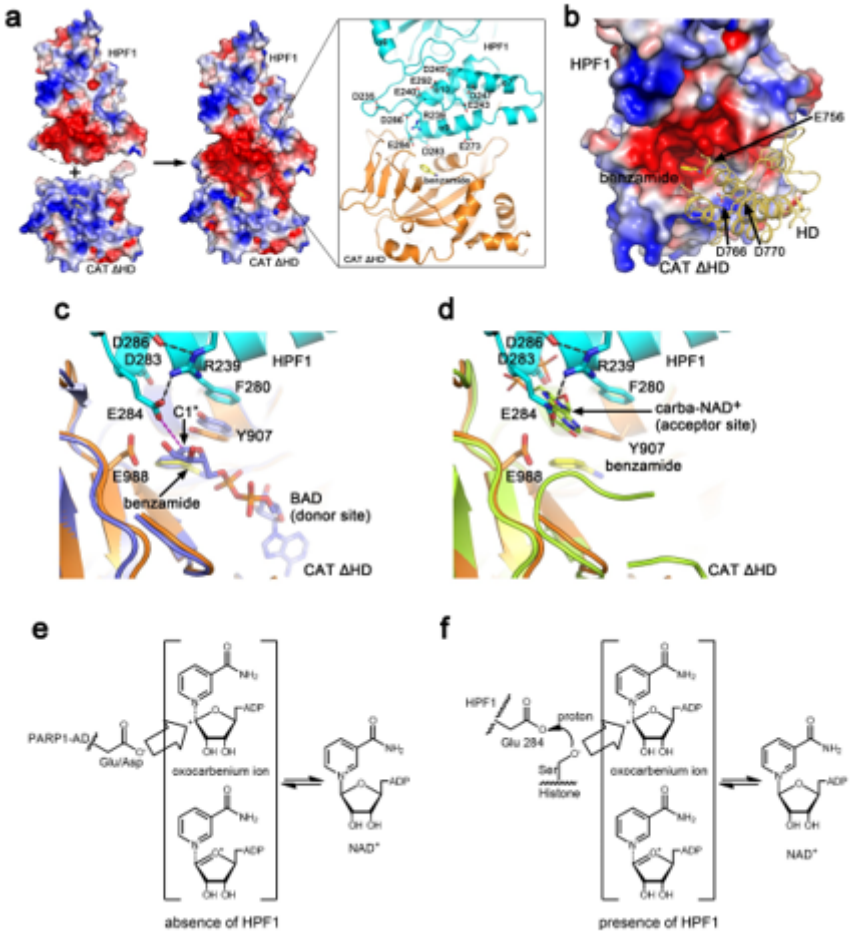

Figure 3

Structural basis of HPF1 function on modulating PAPR1 activity. (a) Surface electrostatic potential of human HPF1, PAPR1-CAT ΔHD and the hetero-dimer. The negatively and positively charged regions are colored red and blue, respectively. A strongly negatively charged region in HPF1 merges to the active site of PARP1-ART in the complex, creating a joint negatively charged active site. The inset on the right shows the acidic and basic residues in this HPF1 negatively charged region. (b) A close view of the remodeled active site and the HD domain if in folded state. The HD domain shown as cartoons here based on superimposition of the HPF1/PAPR1-CAT ΔHD structure ART domain with that in the DNA-bound PARP1 crystal structure (PDB 4DQY). (c) Superimposition of the active site in the HPF1/PAPR1-CAT ΔHD structure (cyan and orange) and that in the previously reported PARP1-ART structure binding to BAD, an NAD+ analog (PDB 6BHV, light-blue)22. (d) Superimposition of the active site in the HPF1/PAPR1-CAT ΔHD structure (cyan and orange) and that in the previously reported carba-NAD+-bound PARP1-CAT structure (PDB 1A26, lime)29. The ADP moiety of carba-NAD+ shown as lime sticks in this figure had been proposed to represent the ADP-ribosylation acceptor in ADPr chain elongation/branching. (e) Proposed catalytic mechanism of PARP1 automodification in the absence of HPF1. Without HPF1, the acidic residues in automodification domain (AD) of PARP1 can access the active center to get ADP-ribosylated. (f) Proposed catalytic mechanism of histone serine in the presence of HPF1. Upon HPF1 binding, HPF1 Glu284 carboxyl is positioned about 4.6Å away from the donor NAD+ (represented by BAD here) ribose. This distance is too far away for Glu284 itself to accept the ADP-ribose, but would work to catalyze ADP-ribosylation of a serine by promoting deprotonation of its sidechain hydroxyl.

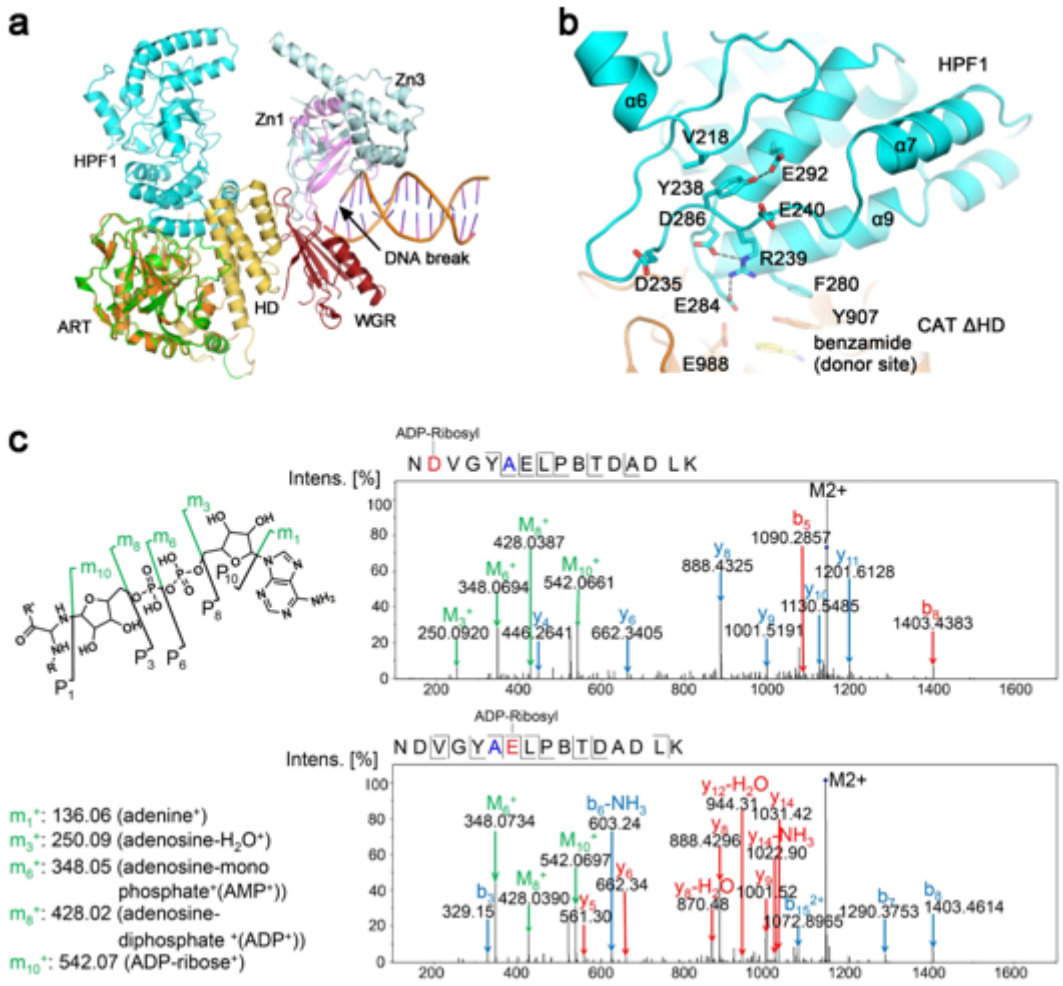

Figure 4

Depicting the function of HPF1 Arg239. (a) Comparison of the HPF1/PAPR1-CAT ΔHD complex structure and the DNA-bound PARP1 crystal structure (PDB 4DQY) 18 by superimposing the ART domains from both (orange – ART determined in this report; green – ART of PDB 4DQY). HPF1 binding to PARP1 would presumably dislodge PARP1 automodification domain (AD) that was previously proposed to locate roughly in the same position as HPF1 binds (see Supplemental Figure S1), thus prevents automodification of PARP1. (b) A close view of the long α6-α7 loop region structure and its relative position to the active center of the HPF1/PARP1 complex. (c) Mass Spectrometry analysis revealed that HPF1 R239A mutation resulted ADP-ribosylation on Asp235 and Glu240, a unique phenomenon only seen for this mutant (see Figure 2B, black arrow). The mutated residue 239 is shown in blue in the sequence, while the modified residues Asp235 and Glu240 are shown in red.

Supplementary Files

This is a list of supplementary files associated with this preprint. Click to download.

- SupplementalInformationv12.docx

- ValidationreportfullHPF1ART.pdf
- ValidationreportfullhHPF1.pdf
- ValidationreportfullmHPF1.pdf